

Infrared Intensities of Bending Fundamentals in Gaseous HCCCN and DCCCN

Masakatsu UYEMURA,* Shuji DEGUCHI,† Yoshikazu NAKADA,† and Takashi ONAKA†

*Department of Industrial Chemistry, Faculty of Engineering, Tokyo Institute of Polytechnics,
Atsugi, Kanagawa 243-02*

†Department of Astronomy, Faculty of Science, The University of Tokyo, Hongo, Bunkyo-ku, Tokyo 113

(Received May 21, 1981)

The infrared spectra of three bending fundamentals (ν_5 , ν_6 , and ν_7) of gaseous cyanoacetylene and cyanoacetylene-*d* have been measured and their integrated absorption coefficients $A(\nu_i)$ have been determined. The spectral pattern of ν_5 fundamental region in HCCCN has been interpreted by assuming the Fermi resonance between $\nu_5=1$ and $\nu_7=3$ states. On the basis of the experimental intensity data and the normal coordinate treatment, the dipole-moment derivatives with respect to the internal bending coordinates have been calculated.

Many spectral data of cyanoacetylene have been obtained from several astronomical sources, and many microwave studies have been reported.¹⁾ Lafferty and Lovas reviewed them to obtain information applicable to radio astronomy.²⁾ Several infrared studies have been reported since Turrell *et al.*'s first work of HCCCN in gaseous, liquid, and crystalline states. Job and King studied the infrared spectra of gaseous HCCCN and DCCCN; they also studied the Raman spectra of liquids. The infrared, far-infrared, and Raman spectra of crystalline HCCCN and DCCCN were reported by Nolin *et al.*³⁾ One of the present authors studied the infrared intensities of the stretching fundamentals in gaseous and crystalline states with special interest in the intensity changes caused by the hydrogen-bond formation.⁴⁾ Recently, Mallinson and Fayt measured the high-resolution spectra of HCCCN and DCCCN in the region of 1800—6500 cm⁻¹, in order to determine the accurate band centers for all seven fundamentals and the rotational constants for three stretching fundamentals, which had not been available from microwave studies.⁵⁾ Their spectrometer, however, was unable to cover the lower frequency region where the three bending fundamentals lie. The present study was undertaken to measure the infrared intensities of the three bending fundamentals of gaseous HCCCN and DCCCN, and thereby to obtain the information concerning the dipole-moment changes due to molecular bending motions.

Experimental

HCCCN was kindly supplied from Takeda Chemical Industries. The methods of purification and deuteration were described previously.⁴⁾

The deuterium content in DCCCN determined from the band intensity of residual HCCCN, was found to be 98%. Spectra of ν_5 and ν_6 fundamentals were obtained using a Perkin-Elmer model 125 spectrometer with a 5 cm path-length cell, and those of ν_7 were obtained using a Hitachi model FIS-21 single beam far-infrared spectrometer with a 10 cm path-length cell equipped with polyethylene windows. The spectral resolution of the spectrometers were from 1.1 cm⁻¹ to 1.6 cm⁻¹ in the ν_5 and ν_6 band regions and about 0.6 cm⁻¹ in the ν_7 band region. In the measurements of ν_5 and ν_6 bands, the sample gas was first admitted to the cell, then Helium gas was added to fill it; the total pressure was about 7×10^4 Pa. The integrated absorption coefficients:

$$A(\nu_i) = \int_{\text{band}} \ln(T_0/T) d\tilde{\nu} \quad (1)$$

were obtained and plotted against to the sample pressure p at 273 K. In the case of ν_7 , the spectra were recorded first with an empty cell, and then with a cell containing the sample gas; the transmittances were calculated point by point. In these measurements, the changes of recording conditions would appreciably affect the apparent spectra, so that relatively large errors would be expected to accumulate in $B(\nu_i)$ if the integration were carried out over the entire band region. Therefore, the integration was carried out over the Q-branch region and then this value was used to obtain the integrated molar absorption coefficient $A(\nu_i)$, as described later.

Results and Discussions

Observed frequencies of the bending fundamentals, their combinations and overtones are given in Table 1, together with those reported previously.^{3,5)} In the ν_5 and ν_6 band regions of HCCCN and DCCCN, two sharp and strong bands were observed, accompanied by some sub-bands. The former were assigned to the Q-branch of $\nu_5=1 \leftarrow 0$ and $\nu_6=1 \leftarrow 0$ transitions. Most of the latter may be assigned to hot bands, on the basis of their intensities relative to the fundamentals and their small frequency shifts from the $\nu_i=1 \leftarrow 0$ transitions, because the bending fundamental frequencies are relatively low in these molecules. In the ν_5 band region of HCCCN, the band at 663.7 cm⁻¹ was assigned to the $\nu_5=1 \leftarrow 0$ transitions, as shown above. The situation here is, however, somewhat different in that the sub-bands shift considerably from the $\nu_5=1 \leftarrow 0$ transition and the intensity of the band at 669.8 cm⁻¹ seems to be appreciably larger than that expected from a hot band (Fig. 1). In order to determine the spectral origin of these sub-bands, the spectra were recorded at different temperatures. As the temperature was changed from 51 °C to -17 °C, the bands at 649.8 cm⁻¹ and 676.9 cm⁻¹ showed an appreciable intensity decrease, whereas the band at 669.8 cm⁻¹ did not show such a change. This observation suggests that the bands at 649.8 cm⁻¹ and 676.9 cm⁻¹ may be attributed to hot bands, but the band at 669.8 cm⁻¹ may not. At this point, it may be noted that the ν_7 fundamental lies at 222.4 cm⁻¹, and hence the $3\nu_7$ band is expected near the ν_5 fundamental. Incidentally, in the $2\nu_5$ band region, two bands were observed at 1313.1 cm⁻¹ and 1340 cm⁻¹; the former is of the parallel type and is much stronger than the latter. These two bands can be assigned to $2\nu_5$ and $\nu_5+3\nu_7$ respectively, if a resonance

TABLE 1. OBSERVED FREQUENCIES OF BENDING FUNDAMENTALS, THEIR OVERTONES AND COMBINATIONS IN GASEOUS CYANOACETYLENE (cm^{-1})

	Job <i>et al.</i> ^{a),c)}	Mallinson <i>et al.</i> ^{b)}	This work ^{c)}
HCCCN			
$\nu_5 + 3\nu_7$ $2\nu_5$	1314		{1340 1313.1
$2\nu_6$	1010		1012
$\nu_5 + \nu_7$	885		
$\nu_6 + \nu_7$	720		719
			676.9 ^{d)}
$3\nu_7$ ν_5	663	663.209	{669.8 663.7 649.8 ^{d)} 514.6 ^{d)}
ν_6	500	498.5	499.2
ν_7		222.402	223.5
DCCCN			
$2\nu_5$	1045		1044.6
$\nu_5 + \nu_6$	1015		1015.2
$2\nu_6$			997.6
$\nu_5 + \nu_7$	723		
$\nu_6 + \nu_7$	702		704
			528.2 ^{d)} 525.2 ^{d)}
ν_5	522	523.008	522.6 505.5 ^{d)}
ν_6	494	494.500	494.6
ν_7		213.000	213.0

a) Ref. 3. b) Ref. 5. Band centers which do not include the $-l^2 B_v$ term. c) Frequencies of the Q-branch maxima in perpendicular bands or those of the minimum absorption between P and R branches in parallel bands. d) Hot band.

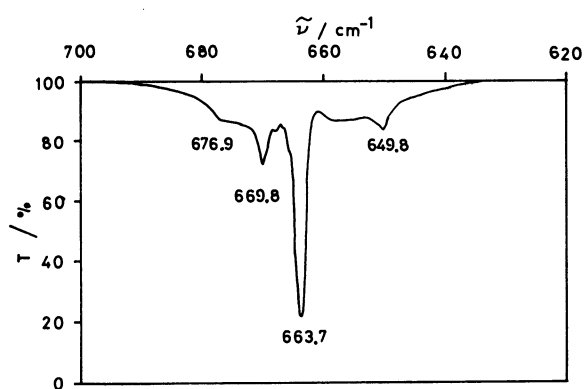


Fig. 1. Spectrum of ν_5 in gaseous HCCCN.

interaction is assumed between $\nu_5=2$ and $\nu_5=1$, $\nu_7=3$ states. Although the existence of the Fermi resonance between $\nu_5=1$ and $\nu_7=3$ in Π symmetry state has not been confirmed from the microwave studies,²⁾ and the origin of the interaction between $\nu_5=2$ and $\nu_5=1$, $\nu_7=3$ states is still open to discussion, the present infrared results may be best interpreted by the energy level diagram shown in Fig. 2, where the Fermi resonance between $\nu_5=1$ and $\nu_7=3$ states is taken into account. According to this energy level diagram, the large

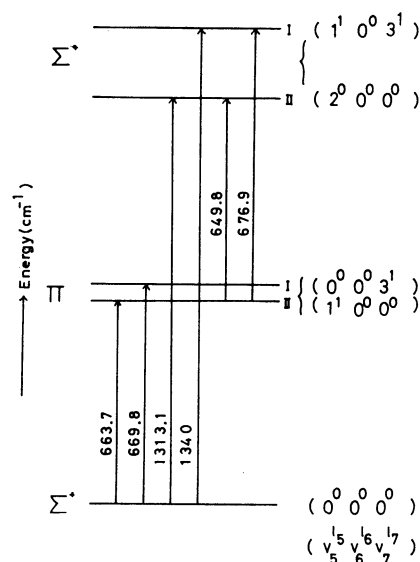


Fig. 2. Energy level diagram involving the excited states of ν_5 and ν_7 in HCCCN.

frequency shifts of the sub-bands are due to the energy splitting in the initial and final states, and the anomalous intensity of the band at 669.8 cm^{-1} is due to the intensity borrowing from ν_5 fundamental. Since the majority of the sub-bands in this region were related to the ν_5 fundamental, the integrated absorption coefficient in this region was ascribed only to the ν_5 fundamental intensity.

In the ν_6 band region of HCCCN, the band at 499.2 cm^{-1} was assigned to the Q-branch of the $\nu_6=1 \leftarrow 0$ transition; the band at 514.6 cm^{-1} was assigned to the Q-branch of the $\nu_6=2 \leftarrow 1$ transition, and the other weaker bands may be assigned to the hot bands originating from other excited states. Therefore, the observed intensities in this region were integrated to give $B(\nu_6)$.

In the case of DCCCN, ν_5 and ν_6 bands were observed to overlap and form a single band envelope. In this region, two strong bands at 522.6 cm^{-1} and 494.6 cm^{-1} were unambiguously assigned to the Q-branches of $\nu_5=1 \leftarrow 0$ and $\nu_6=1 \leftarrow 0$ transitions respectively. In addition to these bands, there appeared some bands of small frequency shifts and low intensities relative to $\nu_5=1 \leftarrow 0$ or $\nu_6=1 \leftarrow 0$ transition, and these may be assigned to a hot band. Then, the intensities in this region were integrated to give an intensity sum $B(\nu_5) + B(\nu_6)$. The method used to separate this sum into individual components will be shown in the later section. Experimental quantities, *i.e.*, $B(\nu_5)$ and $B(\nu_6)$ of HCCCN, and $B(\nu_5) + B(\nu_6)$ of DCCCN, were plotted against to sample pressure p at 273 K , as shown in Fig. 3. Then, the limiting slope at $p \rightarrow 0$ was obtained to give the integrated molar absorption coefficient:

$$A(\nu_i) = \int_{\text{band}} \alpha d\tilde{\nu}. \quad (2)$$

The resultant intensity sum $A(\nu_5) + A(\nu_6)$ in DCCCN was divided by the following method. Since the Q-branch intensity of ν_5 band was close to that of ν_6 , the integrated intensities were divided at the wavenumber halfway between the Q-branch maxima, and $A(\nu_5)$ and

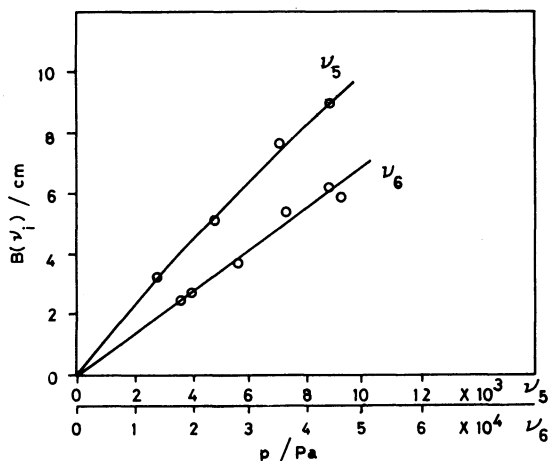


Fig. 3a. Beer's law plots for gaseous HCCCN.

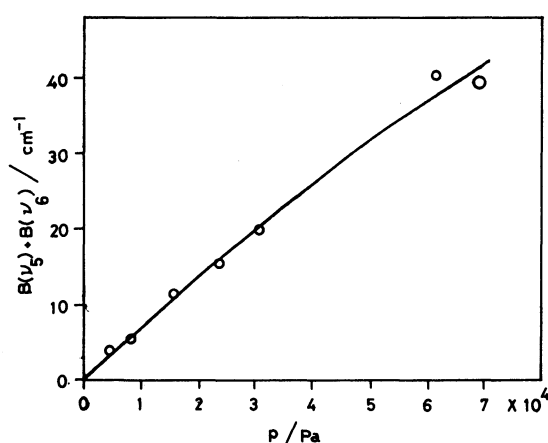


Fig. 3b. Beer's law plots for gaseous DCCCN.

$A(\nu_6)$ were assumed to be proportional to the divided areas of the higher and lower frequency sides. As for the determination of $A(\nu_7)$, the absorption coefficients were integrated over the Q-branch region of ν_6 and ν_7 bands to give $B_Q(\nu_6)$ and $B_Q(\nu_7)$. Then $A(\nu_7)$ was determined from the following expression:

$$A(\nu_7) = A(\nu_6) \times \frac{B_Q(\nu_7)}{B_Q(\nu_6)} \times \frac{p_6}{p_7} \times \frac{l_7}{l_6}, \quad (3)$$

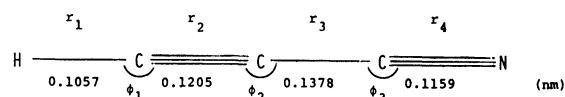
where l_i is the path-length of the gas cell, and p_i stands for the pressure of the sample. The integrated molar absorption coefficients obtained in this study are shown in Table 2.

TABLE 2. OBSERVED INFRARED INTENSITIES OF BENDING FUNDAMENTALS IN GASEOUS CYANOACETYLENE (km mol^{-1})

	$A(\nu_5)$	$A(\nu_6)$	$A(\nu_7)$
HCCCN	68.4	8.0	0.18
DCCCN	21.0	24.5	0.22

Now, let us consider the errors in the resultant intensities. It is well known that among the various sources of error, the relation between the spectral slit-width and the half-width of the pressure-broadened spectra is most important for the determination of $A(\nu_i)$. In the case of ν_5 and ν_6 fundamentals, the Beer's law plots

are seen to be almost linear; this gives the experimental evidence that the relation between the slit-width and the half-width of the spectra was appropriate. Although the Beer's law plots was not available in the ν_7 fundamental, the relation may be regarded as close to that in ν_5 and ν_6 , because the spectral slit-width and the total pressure of the gas in the measurement of ν_7 were nearly half of those in ν_5 and ν_6 . It is also well known that the half-width of a spectral line is proportional to the pressure of gas when the pressure broadening is the dominant factor for the line-width. The errors in $A(\nu_i)$ may be estimated at 15% for ν_5 and ν_6 , and 25% for ν_7 , based on the estimation of the errors in the intensities of the stretching fundamentals in gaseous states.



$$s_1 = \Delta r_1 \quad s_2 = \Delta r_2 \quad s_3 = \Delta r_3 \quad s_4 = \Delta r_4$$

$$s_5 = (r_1 r_2)^{1/2} \Delta \phi_1 \quad s_6 = (r_2 r_3)^{1/2} \Delta \phi_2 \quad s_7 = (r_3 r_4)^{1/2} \Delta \phi_3$$

Fig. 4. Molecular structure and internal coordinates.

In order to obtain L^{-1} matrix elements which are necessary for the conversion of $(\partial \mu / \partial Q_i)$ to the dipole-moment derivatives with respect to internal coordinates $(\partial \mu / \partial S_j)$, the force constants for bending vibrations were determined by a least squares method based on the frequency data by Mallinson *et al.*⁵⁾ The force constants for stretching vibrations were determined by the same method. The molecular geometry and internal coordinates used are shown in Fig. 4. It is not practical to assume a general valence force field, because the number of the observed frequencies in HCCCN and DCCCN are limited to eight in the stretching vibration and six in the bending vibration, so that the following potential function was used;

$$2V = K_1 \Delta r_1^2 + K_2 \Delta r_2^2 + K_3 \Delta r_3^2 + 2K(\Delta r_2 \Delta r_3 + \Delta r_3 \Delta r_4) + H_1 r_1 r_2 \Delta \phi_1^2 + H_2 r_2 r_3 \Delta \phi_2^2 + H_3 r_3 r_4 \Delta \phi_3^2 + 2H \sqrt{r_1 r_3} r_2 \Delta \phi_1 \Delta \phi_2, \quad (4)$$

where K stands for the interaction between $\text{C}\equiv\text{C}$ stretch and $\text{C}-\text{C}$ stretch, and also for that between $\text{C}-\text{C}$ stretch and $\text{C}\equiv\text{N}$ stretch, whereas H stands for the interaction between HCC bend and CCC bend. When other forms of the function were assumed, the resultant force constants diverged or gave large correlation factors. The force constants, and the calculated and observed frequencies are shown in Table 3, where a fairly good agreement is obtained between them. The largest correlation factor is 0.86 for the element between K_4 and K . Then, $(\partial \mu / \partial S_j)$ were calculated by the following expression, using $(\partial \mu / \partial Q_i)$ and L^{-1} matrix elements obtained above:

$$(\partial \mu / \partial S_j) = \sum_k (\partial \mu / \partial Q_k) L_{jk}^{-1}. \quad (5)$$

It is well known that $(\partial \mu / \partial S_j)$ derivatives obtained from Eq. 5 include some contribution due to molecular rotation, if S_j and overall rotation belong to the same symmetry species.^{6,7)} This is the case for the bending vibration of these molecules, so that the derivatives

TABLE 3a. FORCE CONSTANTS OF GASEOUS CYANOACETYLENE (10^2 N m^{-1})

	Force constants	(Dispersion)
K_1	5.924	(0.027)
K_2	15.93	(0.15)
K_3	6.673	(0.126)
K_4	17.21	(0.30)
K	0.607	(0.090)
H_1	0.1882	(0.0015)
H_2	0.1643	(0.0043)
H_3	0.2224	(0.0038)
H	0.0672	(0.0026)

TABLE 3b. CALCULATED FREQUENCIES OF GASEOUS CYANOACETYLENE (cm^{-1})

	HCCCN		DCCCN	
	Mallinson ^{a)}	Calculated	Mallinson ^{a)}	Calculated
ν_1	3327.372	3332.2	2608.520	2600.3
ν_2	2273.996	2279.6	2252.155	2246.7
ν_3	2079.306	2083.1	1968.329	1967.0
ν_4	863.5	863.9	850.3	849.7
ν_5	663.209	664.2	523.008	521.8
ν_6	498.5	500.3	494.500	492.7
ν_7	222.554	222.2	213.000	213.0

a) Ref. 5. Band centers which do not include the $-l^2 B_V$ term.

obtained from HCCCN and DCCCN are designated as $(\partial\mu/\partial S_j)_H$ and $(\partial\mu/\partial S_j)_D$, because the effect of the compensating rotation is different for different isotopes. In order to compare these derivatives on the same basis, a reference molecule was assumed, where the mass of hydrogen atom is supposed to be zero. Then, it can be shown that the experimental quantities $(\partial\mu/\partial S_j)_H$ and $(\partial\mu/\partial S_j)_D$ are related to $(\partial\mu/\partial S_j)_R$ in this reference molecule by the following expression:

$$(\partial\mu/\partial S_j)_R = (\partial\mu/\partial S_j)_H - (\partial\mu/\partial S_j)_{R,H}^{\text{corr}}, \quad (6a)$$

$$(\partial\mu/\partial S_j)_R = (\partial\mu/\partial S_j)_D - (\partial\mu/\partial S_j)_{R,D}^{\text{corr}}, \quad (6b)$$

where $(\partial\mu/\partial S_j)_{R,H}^{\text{corr}}$ and $(\partial\mu/\partial S_j)_{R,D}^{\text{corr}}$ stand for the rotational corrections. These correction terms can be calculated by the following expression:

$$(\partial\mu/\partial S_j)_{R,i}^{\text{corr}} = \sum_{s=1}^{3N-6} (\partial\mu/\partial x_s) \sum_{n=1}^6 (\alpha_R)_{s,n} \left[\sum_{t=1}^{3N} (\beta_R)_{n,t} (A_i)_{t,j} \right], \quad (7)$$

$i = H, D$

where μ is the molecular permanent dipole-moment and A , β , and α are the matrices relating the Cartesian displacement coordinates x with the internal coordinates S and the coordinates of translation and rotation ρ :

$$x_s = \sum_{k=1}^{3N-6} (A_i)_{s,k} S_k + \sum_{n=1}^6 (\alpha_i)_{s,n} (\rho_i)_n, \quad (8a)$$

$$S_k = \sum_{s=1}^{3N-6} B_{k,s} x_s, \quad (\rho_i)_n = \sum_{s=1}^{3N} (\beta_i)_{n,s} x_s, \quad i = H, D \quad (8b)$$

Since the signs of $(\partial\mu/\partial Q_i)$ are not determinable experimentally, all possible sign combinations in $(\partial\mu/\partial Q_i)$ are shown in Table 4, together with the rotational correction terms. It may be seen from the table that the sign combinations $(+ - +)$ and $(+ - -)$ with the correction term subtracted give better agreement between HCCCN and DCCCN: $(+ - -)$ gives the

TABLE 4a. CALCULATED VALUES OF THE ROTATIONAL CORRECTION TERM^{a)} (D/A)

	S_5	S_6	S_7
HCCCN	-0.11	-0.11	-0.05
DCCCN	-0.19	-0.21	-0.10

a) Calculated using $\mu = 3.724 \text{ D}$ (Ref. 2). The positive direction of the dipole-moment change caused by atomic displacements is shown in Fig. 5.

TABLE 4b. POSSIBLE COMBINATIONS OF RELATIVE SIGNS IN $(\partial\mu/\partial Q_5, \partial\mu/\partial Q_6, \partial\mu/\partial Q_7)$ (D/A)

	+++	+-+	++-	---
(Rotational correction term added)				
S_5 {	HCCCN -0.74	-0.79	-0.71	-0.76
	DCCCN 0.02	-0.72	0.08	-0.66
S_6 {	HCCCN -0.01	-0.47	0.21	-0.25
	DCCCN 0.55	-0.29	0.83	-0.01
S_7 {	HCCCN -0.43	0.36	-0.25	0.54
	DCCCN -0.90	0.39	-0.70	0.59
(Rotational correction term subtracted)				
S_5 {	HCCCN -0.96	-1.01	-0.93	-0.98
	DCCCN -0.36	-1.10	-0.30	-1.04
S_6 {	HCCCN -0.23	-0.69	-0.01	-0.47
	DCCCN 0.13	-0.71	0.41	-0.43
S_7 {	HCCCN -0.53	0.26	-0.35	0.44
	DCCCN -1.10	0.19	-0.90	0.39

best agreement in $(\partial\mu/\partial S_5)_R$ and $(\partial\mu/\partial S_7)_R$, whereas $(+ - +)$ gives the best agreement in $(\partial\mu/\partial S_6)_R$. It may be pointed out here that the observed $(\partial\mu/\partial S_6)_R$ may contain a larger error than the others, because $A(\nu_7)$ is expected to contain the largest error in the three bending fundamentals and it gives the largest contribution to $(\partial\mu/\partial S_6)_R$. Therefore, the difference of $(\partial\mu/\partial S_6)_R$ in $(+ - -)$ may be ascribed to the experimental error. In view of the above discussions, it seems most reasonable to take the $(+ - -)$ sign combination with the correction term subtracted as the most preferable one. In order to determine the direction of the rotational correction term, it is necessary to know the direction of the permanent dipole-moment μ . For this purpose, the semi-empirical SCF calculation was carried out and the dipole-moment μ was obtained to be 2.93 D, with the polarity of $\text{H}^+\text{C}\equiv\text{C}\text{N}^-$. This polarity agrees with that expected from the generally accepted bond polarities of $\text{H}-\text{C}$ and $\text{C}\equiv\text{N}$. The rotational correction terms

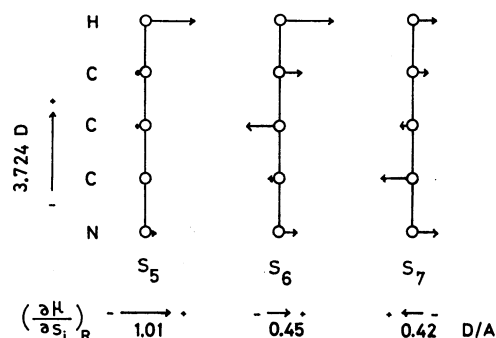


Fig. 5. Atomic displacements along internal coordinates and changes of dipole-moment.

were calculated from the dipole-moment of 3.724 D derived from the microwave studies²⁾ with the polarity of H^+CCCCN^- . The experimentally determined relative signs in $(\partial\mu/\partial S_i)_R$ and $(\partial\mu/\partial S_i)_{R,\text{HCD}}^{\text{corr}}$ then lead to the determination of the direction of each $(\partial\mu/\partial S_i)_R$. The atomic displacements along each internal coordinate and the resultant changes of the dipole-moment are shown in Fig. 5. It may be noted that $(\partial\mu/\partial S_5)_R$ of cyanoacetylene and $(\partial\mu/\partial S_2)_R$ of hydrogen cyanide have same direction and their values are close, i.e., the value of $(\partial\mu/\partial S_2)_R$ in hydrogen cyanide after the rotational correction has been taken into account is 1.08 D/A. It can be seen from the B matrix elements for each internal coordinate that both dipole-moment derivatives are due to the displacement of hydrogen atoms. Therefore, the close agreement between them may be regarded as the experimental evidence of the similar nature of the H-C bond in these molecules. Though it does not seem so simple to relate the dipole-moment derivatives to each bond polarity of molecule, as in the case of $(\partial\mu/\partial S_5)_R$, the dominant part of $(\partial\mu/\partial S_7)_R$ may be due to the $\text{C}\equiv\text{N}$ bond which has a high polarity of $\text{C}^+\equiv\text{N}^-$.

The authors wish to express their thanks to Professor Shiro Maeda and Professor Chiaki Hirose of Tokyo Institute of Technology for helpful discussions and

encouragements. The normal coordinate calculations and the semi-empirical SCF (CNDO) calculations were carried out at the Computer Center, the University of Tokyo.

References

- 1) S. Deguchi, Y. Nakada, T. Onaka, and M. Uyemura, *Publ. Astron. Soc. Jpn.*, **31**, 105 (1979).
- 2) W. J. Lafferty and F. J. Lovas, *J. Phys. Chem. Ref. Data*, **7**, 441 (1978).
- 3) G. C. Turrell, W. Johns, and A. Maki, *J. Chem. Phys.*, **26**, 1544 (1957); V. A. Job and G. W. King, *Can. J. Chem.*, **41**, 3132 (1962); C. Nolin, J. Weber, and R. Savoie, *J. Raman Spectrosc.*, **5**, 21 (1976).
- 4) M. Uyemura and S. Maeda, *Bull. Chem. Soc. Jpn.*, **47**, 2930 (1974).
- 5) P. D. Mallinson and A. Fayt, *Mol. Phys.*, **32**, 473 (1976).
- 6) J. Overend, "Infrared Spectroscopy and Molecular Structure," ed by M. Davis, Elsevier Publ. Co., Amsterdam (1963), p. 374.
- 7) B. Crawford, Jr., *J. Chem. Phys.*, **20**, 977 (1952); A. D. Dickson, I. M. Mills, and B. Crawford, Jr., *ibid.*, **27**, 445 (1957).
- 8) M. Uyemura and S. Maeda, *Bull. Chem. Soc. Jpn.*, **45**, 1081 (1972).
- 9) E. B. Wilson and A. T. Wells, *J. Chem. Phys.*, **14**, 578 (1946).
- 10) J. A. Pople and G. A. Segal, *J. Chem. Phys.*, **43**, s 136, (1965); **44**, 3289 (1966).